LPS-SQUALENE INTERACTION ON D-GALACTOSE INTESTINAL ABSORPTION

Mª José FELICES[1], Sara ESCUSOL[1], Roberto MARTINEZ-BEAMONTE[2, 3], Sonia GASCÓN[1, 3], Cristina BARRANQUERO[2, 3], Cristina SANCHEZ-DE-DIEGO[4], Jesús OSADA[2, 3] and Mª Jesús RODRÍGUEZ-YOLDI[1, 3*]

[1]Dept. of Pharmacology and Physiology, [2]Dept. of Biochemistry, Molecular and Cellular Biology, Veterinary Faculty, University of Zaragoza, 50013 Zaragoza, Spain.

[3]CIBERobn (ISCIII), IIS Aragón, IA2, Zaragoza, Spain.

[4]Dept. Physiological Sciences II. University of Barcelona, Barcelona, Spain.

[*]Corresponding author: M. J. Rodriguez-Yoldi,

Physiology, Veterinary Faculty,

Miguel Servet 177, 50013 Zaragoza, Spain.

Phone: 34-976 761649. Fax: 34-976 761612.

e-mail: mjrodyol@unizar.es

Running head**:** LPS-squalene interaction.

Abstract

The dynamic and complex interactions between enteric pathogens and the intestinal epithelium often lead to disturbances in the intestinal barrier, altered fluid, electrolyte and nutrient transport and can produce an inflammatory response. Lipopolysaccharide (LPS) is a complex polymer forming part of the outer membrane of Gram negative bacteria. On the other hand, squalene is a triterpene present in high levels in the extra virgin olive oil that has beneficial effects against several diseases and it has also anti-oxidant and anti-inflammatory properties. The aim of this work was to study whether the squalene could eliminate the LPS effect on D-galactose intestinal absorption in rabbits and Caco-2 cells. The results showed that squalene reduced the effects of LPS on sugar absorption. High LPS doses increased D-galactose uptake through paracellular via but also decreased the active sugar transport because the SGLT1 levels were disminished. However, the endotoxin effect on paracellular way seemed to be more important than on the transcellular route. At the same time, an increased in RELM-β expression was observed. This event could be related to inflammation and cause a decrease of SGLT1 levels. In addition, MLCK protein is also increased by LPS and this event could be related to the increase of sugar transport through *tight junctions*. At low doses, the LPS could inhibit SGLT1 intrinsic activity. Bioinformatic studies by docking confirm the interaction between LPS-squalene which could occur through MLCK and SGLT-1 proteins.

Key words: LPS, squalene, intestinal-absorption, SGLT1, RELM-β, MLCK

Introduction

Intestinal mucosal surfaces are lined by epithelial cells. These cells establish a barrier between potentially hostile external environments and the internal milieu. However, intestinal mucosae is also responsible for nutrient absorption and waste secretion, thus requiring a selectively permeable barrier. These functions place the mucosal epithelium at the centre of interactions between the mucosal immune system and luminal contents, including dietary antigens and microbial products [34].

The intestinal epithelium involves selective permeability through 2 major routes: transepithelial/transcellular and paracellular pathways [33]. Transcellular permeability is generally associated to solute transport through the epithelial cells, and predominantly regulated by selective transporters for amino acids, sugars, short-chain fatty acids, and electrolytes [12]. Paracellular permeability is associated with transport through the space between epithelial cells, and is regulated by intercellular complexes localized at the apical-lateral membrane junction and along the lateral membrane [24].

The dynamic and complex interactions between enteric pathogens and the intestinal epithelium often lead to disturbances in the intestinal barrier, altered fluid and electrolyte transport and the induction of an inflammatory response [5].

Lipopolysaccheride (LPS), a constituent of the cellular wall of gram negative bacterial, can act as an endotoxin and can be responsible for septic syndrome [41]. This endotoxin and its derived cytokines are capable of modulating the intestinal tight junction (TJ) permeability by signal transduction pathway activation [2]. Thus, Nighot et al. have shown that myosin light chain kinase (MLCK) plays a central role in the LPS-induced increase in TJ permeability [25]. Likewise, the transcellular pathway can also be regulated by LPS and its cytokines acting on the specific proteins related to sugars and amino acids transport [42]. In this respect, previous studies in our laboratory have shown that LPS altered the intestinal absorption of amino acids and sugars *in vivo* and *in vitro* by modifying the expression of their respective carriers [15,3,4]. In addition, the cytokines released by endotoxins, tumour necrosis factor alpha (TNF-α) and interleukin 1 beta (IL-1β) have shown an inhibitory effect on L-leucine, D-galactose and D-fructose intestinal absorptions [15,3]. These effects could be related to activation of multiple intracellular signalling cascades including the mitogen-activated protein kinase (MAPK) and nuclear factor κB (NF-κB) signal transduction pathway [13,14].

On the other hand, the Mediterranean diet is inspired by the eating habits of countries of the Mediterranean area. Olive oil may be the main health-promoting component of this diet and there is preliminary evidence that regular consumption of olive oil can reduce mortality by decreasing the risk of diseases such as cardiovascular diseases, cancer, neurodegeneration, arthritis and several chronic diseases [27].

In this way, squalene is a triterpene present in high levels in the extra virgin olive oil. This triterpene, together with phenolic compounds, is responsible for its stability. In addition, several studies have shown that squalene has beneficial effects against atherosclerosis and has anti-inflammatory properties. It behaves as an antioxidant [38], that might play an important role preventing ageing and skin pathologies. Squalene is also used as adjuvant in vaccines and in other fields such as cancer [23].

For all this, the aim of this work was to study whether the squalene present in the diet of the animals or added to cells was able to modify the effects induced by LPS on the intestinal absorption of galactose sugar.

We have used two experimental models: rabbit jejunum and Caco-2 cells. We have used cells in order to see the effect of LPS and squalene in intestinal tissue free of nervous and/or hormonal signals which are present in the animal model. These cells differentiate into polarized monolayer such that their phenotype, morphologically and functionally, resembles that of the small intestinal epithelial cells. They develop the morphological characteristics of mature enterocytes [8].

Materials and Methods

Materials

D-galactose, D-mannitol, Hepes, Tris (hydroxymethyl) amino-methane, bovine serum albumin, dimethyl sulfoxide (DMSO), lipopolysaccharide from *E. coli* (LPS) serotype 0111:B4, squalene and anti-actin were obtained from Sigma (Spain). D-[U-^{14}C] galactose and Biodegradable Counting Liquid Scintillation were obtained from GE Healthcare Life Sciences. The membrane filters were provided by Millipore. The reagents used in Western blot analysis were obtained from Bio-Rad, Sigma and Serva (Spain)

Animals, diets and preparation of intestinal tissue

The experimental animals were housed, handled, and euthanized according to European Union Legislation 86/609/EEC. All experimental protocols were approved by the Ethical Committee of the University of Zaragoza (PI47/10).

During 4 weeks, two groups of six male New Zealand rabbits were fed with a chow diet enriched with 1% of sunflower oil for the control group, and with 1% of sunflower oil and 0.5% of squalene for the squalene group. After this period, the rabbits were treated with LPS using two different regimens of administration: acute (intravenous administration –iv- of LPS through the lateral ear vein, 90 min prior to the sample collection) and chronic (the endotoxin was released for one week by intraperitoneal -ip- osmotic pump implantations) treatments. The animals, then, were divided in four groups: control with/without LPS and squalene with/without LPS. During the treatment, the solid intake, body weight and rectal temperature of the animals were controlled.

Rabbits were euthanized following previously published protocols [13]. Intestinal samples were then taken and the proximal jejunum was removed and rinsed with ice-cold Ringer's solution which contained (in mM): 140 NaCl, 10 $KHCO_3$, 0.4 KH_2PO_4, 2.4 K_2HPO_4, 1.2 $CaCl_2$ and 1.2 $MgCl_2$, pH 7.4.

Sugar uptake measurements in rabbit jejunum

Tissue uptake

Rings of everted jejunum weighing about 100 mg were continuously bubbled with 95% O_2 - 5% CO_2. Tissue rings were incubated for 3 min in Ringer's solution at 37ºC containing 0.01 µCi/ml D-[U-^{14}C] galactose plus 0.5 mM unlabeled substrate. After incubation, tissue pieces were washed with three gentle shakes in ice-cold Ringer's solution and blotted carefully on both sides to remove excess of solution. Tissues were then weighed, and incubated overnight in 0.5 ml of 0.1 M HNO_3 at 4ºC to extract the labeled galactose. Aliquots of 200 µl from extract and bathing solutions were counted in 2 ml of biodegradable scintillation fluid. The incubation time of tissue with galactose was 3 min. The measurements were expressed as µmol of D-galactose per gram of tissue.

Cell culture

The Caco-2 cell line PD7 clone was kindly provided by Dr. Edith Brot-Laroche (Université Pierre et Marie Curie-Paris 6, UMR S 872, Les Cordeliers France). Caco-2 cells were maintained in a humidified atmosphere of 5% CO_2 at 37ºC. Cells were grown in Dulbecco's Modified Eagles medium (DMEM) (Gibco Invitrogen, Paisley, UK) supplemented with 20% foetal bovine serum (FBS), 1% nonessential amino acids, 1% penicillin (1000 U/ml), 1% streptomycin (1000 mg/ml) and 1% amphoterycin (250 U/ml). The cells were passaged enzymatically with 0.25% trypsin-1 mM EDTA and sub-cultured on 25 or 75 cm^2 plastic flasks at a density of $2x10^4$ cells cm^{-2}. Culture medium was replaced every 2 days. Cell confluence (80%) was confirmed by microscopic observation. Experiments were performed 17-21 days post-seeding.

For cell treatment studies, cells were seeded in 24-well plates at a density of $4x10^4$ cells/well. The culture medium was replaced with fresh medium (without FBS) containing LPS at concentrations of 50 and 75 µg/ml and/or 50 µM squalene, at preincubation time of 24 h [17]. Once the cells were treated with LPS and/or squalene for 24 h, to medium was added cold and labeled D-galactose for 15 min. The samples taken from the medium and from the cells were measured by radioactive counting.

Determination of cytotoxicity, MTT assay

Cell proliferation inhibition was measured using the MTT [35]. This assay is dependent on the cellular reduction of 3-(4,5-dimethyl-2-thiazoyl)-2,5-diphenyltetrazolium bromide (MTT) by the mitochondrial dehydrogenase of viable cells to a blue formazan product which can be measured spectrophotometrically. Following appropriate incubation of cells, with or without LPS and/or

squalene, MTT was added to each well. The incubation was continued at 37ºC for 3 h, medium was then removed by inversion and 100 µl of DMSO per well were added. At the end, absorbance was measured with a scanning multiwell spectrophotometer at wavelength of 560/670 nm.

Galactose uptake in Caco-2 cells

The medium used as uptake buffer contained 0.5 mM D-galactose with 0.01 µCi/ml D-[U-^{14}C] galactose, and was diluted in Krebs modified buffer (mM: 137 NaCl, 4.7 KCl, 1.2 KH_2PO_4, 1.2 $MgSO_4$, 2.5 $CaCl_2$, Hepes pH 7.2, 4 Glutamine and 0.1 mg/ml BSA). After preincubation time, the cells were incubated for 15 min at 37ºC, and uptake was stopped with ice cold free-substrate buffer with 50 mM D-galactose followed by aspiration. Cells were again washed twice with ice-cold buffer to eliminate non-specific radioactivity fixation and were finally solubilised in 0.1 N NaOH for 24 h. Samples (200 µl) were taken to measure radioactivity by liquid scintillation counting. Protein concentration was determined by the Bradford method (Bio-Rad Protein Assay, Bio-Rad laboratories, Hercules, CA). Measurements were expressed as µmol of D-galactose per mg protein.

Western blotting in BBMV and homogenate

In the study with animals, brush border membrane vesicles (BBMVs) and homogenate were prepared from rabbit jejunum using the Mg^{2+} EGTA precipitation method [14]. The intestine came from the different groups of animals indicated before. Protein content was measured with the Bradford method using bovine serum albumin as standard.

Cells grown on 75 cm^2 plastic flasks were incubated for 24 h, in presence or absence of LPS and/or squalene. After the incubation period, BBMVs and homogenates were isolated [9]. A phosphatase inhibitor cocktail B (Santa Cruz Biotechnology sc-45045) was used in cell extracts (BBMV and homogenate). The protein content was determined by the Bradford method.

The same amounts of vesicles and homogenates protein (20 µg) from control and treated animals or cells were solubilised in Laemmli sample buffer and resolved by 8% SDS-PAGE. Proteins were transferred onto PVDF membranes using a semidry transblot transfer apparatus (Bio-Rad). The protein transfer efficiency was controlled by staining with Ponceau S and by the transfer of Precision Plus Protein Dual Color Standards (Biorad). The following primary antibodies were

used: rabbit polyclonal anti-SLC5A1 (SGLT1) (Abnova, H00006523-D01P), anti-rabbit polyclonal RELM beta (Biorbyt, orb100867) and human monoclonal anti-MLCK (Millipore, MABT194). The following secondary antibodies coupled to peroxidase were used: goat anti-mouse (Millipore AP200P) and rabbit anti-goat (Sigma A5420). Membranes were exposed to autoradiography film, Blue UltraCruz (Santa Cruz Biotechnology) for several time periods to achieve signal intensity within the dynamic range of quantitative detection, and films were scanned at a 600-dpi resolution (via AGFA Arcus II). Intensity of bands for each condition was calculated using Quantity One software version 4.5.0. (BioRad).

Protein modelling

The sequence of rabbit SGLT1 and MLCK were retrieved from Uniprot (http://www.uniprot.org/) entries P11170 and P29294 respectively, and submitted to the online server Robetta for structure modelling (http://robetta.bakerlab.org/) [32]. Robetta provides both *ab initio* and comparative models of protein domains. Firstly, protein chains were parsed into putative domains and aligned with template PDBs. Domains without a detectable PDB homolog were modelled with the Rosetta de novo protocol [31]. Alignments were clustered and comparative models were generated using the RosettaCM protocol [32]. Obtained structures were validated using ProSA-web (https://prosa.services.came.sbg.ac.at/prosa.php) [40] and ModEval (https://modbase.compbio.ucsf.edu/evaluation/). MOdEval was run using MatchBySS training set. Ramachandran Plot was assessed using RAMPAGE

Docking

For SGLT1, docking step was performed using the molecular docking program SwissDock web service (http://www.swissdock.ch/) (Grosdidier, Zoete, & Michielin, 2011b) which uses calculations performed in the CHARMM force field with EADock DSS24 [16]. The ligand and receptor files in the appropriate formats were uploaded to the web-based server for docking study. For the receptor, we used the obtained PDB from the protein modelling step. Ligands files were obtained from Zinc database (**http://zinc.docking.org/**). The structures of the ligands used were ZINC06845904 for squalene and ZINC38377593 for Lipopolysaccharide. Docking was performed using the 'Accurate' parameter with no region of interest defined (blind docking approach). Flexibility for side chains was set at 0 Å within of any atom of the ligand in its reference binding.

Simultaneously, CHARMM energies of the interactions were estimated on the grid [16]. Results were downloaded and visualized in UCSF Chimera package (http://www.rbvi.ucsf.edu/chimera) [26].

Since docking step for MLCK was not supported by Swissdock due to the large size of the protein, RosettaLigand server was used for protein-ligand docking with MLCK (**http://rosie.rosettacommons.org/ligand_docking** [11]. RosettaLigand uses Monte Carlo minimization algorithms to model the rigid body position and orientation of the ligand as well as side-chain conformations of the protein. Then, ensembles of ligand conformations and protein backbones were used to model conformational flexibility. Finally, the models produced are evaluated with a scoring function that includes an electrostatics model, an explicit orientation-dependent hydrogen bonding potential, an implicit solvation model, and van der Walls interactions. Docking experiments were run in triplicate and only clusters with conserved positions in all the experiments were considered for further analysis.

Statistical Analysis

All results were expressed as means ± SE. Means were compared using a one-way analysis of variance (ANOVA). Significant differences at $p<0.05$ was compared using a Bonferroni's multiple and Mann-Whitney-two-tailed comparison tests. The statistical analysis and the graphics were performed using the GraphPad Prism Version 5.02 program on a PC computer.

Results and Discussion

Infections by Gram-negative bacteria generally involve alterations in gastrointestinal function. LPS produces, among other effects, alterations in intestinal transport. In this sense, its effect on the transport of water and electrolytes in various animal species has been studied [18]. In relation to the absorption of nutrients, it has been shown that LPS alters absorption of sugars and amino acids [14,3].

On the other hand, preclinical studies have shown that extra virgin olive oil, fat typical of the Mediterranean diet, has anti-inflammatory, anti-proliferative and anti-apoptotic effects. The beneficial effects of this oil have been attributed to unsaturated fatty acids present in the majority fraction of olive oil. However, the oil contains minor components, with important biological properties, which are included in the unsaponifiable fraction extracted with solvents after saponification of the oil. Squalene is the unsaponifiable compound that is found in a greater proportion and is considered the most important of the oil due to its potential preventive power against cancer, antioxidant, atherosclerosis, skin pathologies, etc. [22].

Some studies have shown that a diet rich in unsaponifiable components of olive oil reduces the damage caused by acute colitis [29] and inhibits the inflammatory response to LPS. In this sense, the anti-inflammatory effect of squalene has been demonstrated by reducing the intracellular levels of inflammatory enzymes and cytokines in neutrophils, monocytes and mouse and human macrophages and in acute colitis in mice [6].

Therefore, the objective of this work was to study whether a diet rich in squalene in animals or the addition to intestinal cells of triterpene could modify the effect of LPS in relation to the intestinal absorption of D-Galactose.

Animal model

Rabbits and diet intervention

Two groups of rabbits were fed during 4 weeks with a chow diet enriched with 1% of sunflower oil for the control group, and with 1% of sunflower oil and 0.5% of squalene for the squalene group. After this period of time, half of the two groups of animals were treated with LPS in

two different ways, acute (90 min by intravenous administration) or chronic (one week by osmotic pump). The last week of the dietetic intervention, the animals were sacrificed and the intestinal samples were excised.

The diet for 4 weeks with squalene did not modify neither the feed intake, nor the weight of the animal (data not shown). The LPS produced an increase in the body temperature of the animals, being this effect diminished, in part, by the squalene in the diet (Figure 1, panels a and b). This event could be due to the existence of a possible interaction of squalene with LPS, perhaps through the proteins like prostaglandins as it has been shown in the literature [29].

D-galactose intestinal absorption

Previous studies in our laboratory have shown an inhibitory effect of LPS (0.02 to 2 μg/kg bw) on intestinal absorption of sugars and amino acids and that at high doses (20 μg/kg bw) produced an important septic state that also affected the absorption of nutrients [14].

Intravenous administration of LPS 6 μg/kg bw (90 min) or the chronic treatment with 1 mg/kg bw for a week, produced an increase in intestinal absorption of D-galactose. This effect was not observed in the group fed the squalene diet and treated with LPS (Figures 3a and 4a).

It is well known that sugars are transported through the brush border by transport systems Na^+-independent and Na^+-dependent, the latter being electrogenic. D-glucose lumen stimulates the synthesis of SGLT1 in the small intestine cells of rats and humans through a cascade of intracellular events, which allow the insertion of functional SGLT1 proteins into the brush border membrane of the enterocytes [30]. On the other hand, the decrease in sugar levels in the lumen reduced the levels of SGLT1 [36].

To determine whether or not the transport system (s) affected by the LPS, we measured the expression of the Na^+ -dependent protein SGLT1 by Western blot. Na^+-independent transport is carried out through the GLUT-2 transporter, which is blocked by floretin and cytochalasin B [10]. This transporter can be expressed in the brush border membrane under certain circumstances, but previous studies carried out by our group showed that it is not expressed in our experimental conditions [13].

Significant differences were observed in the expression of the SGLT1 protein in the different groups of animals (Figures 3b and 4b). LPS decreased the protein levels of SGLT1. This effect was reversed by feeding squalene.

At the same time, we observed an increased in the Resistin-like molecule-β (RELM-β) protein expression. This increase was only significant in the case of the acute treatment of rabbits with LPS (Figures 3c and 4c). The family of RELM-β proteins is involved in insulin resistance, diabetes and inflammatory processes. In addition, it reduces the activity and quantity of the SGLT1 transporter [37,21].

In our results we have seen that the absorption of D-galactose was increased which could indicate a change in the permeability of the paracellular pathways by the action of endotoxin. In this sense, several works, *in vitro* and *in vivo*, have shown that LPS increases permeability through narrow junctions [17].

Therefore, we found interesting to determine the amount of the myosin light chain kinase (MLCK) located at the periphery of the actin-myosin ring and related to changes in membrane permeability. Several studies have shown that an increase of this protein produces a greater permeability in Caco-2 cells, and it is related to sodium-dependent nutrient transporters [7]. We found a significant increase in MLCK protein in the groups of animals treated with LPS (Fig. 3d and 4d) which could justify the greater intestinal absorption of the sugar found (Fig. 3a and 4a). In this case, LPS effect was also reversed by squalene present in the diet.

Cell model (Caco-2 cells in culture)

In addition to using the rabbit as an experimental model, human colon adenocarcinoma cells (Caco-2) were used to carry out transport studies with D-galactose. The Caco-2 cell line is formed by human colon adenocarcinoma cells that, upon reaching the confluence, form a monolayer of polarized cells that present a brush edge structure with narrow junctions at their apical pole. This brush border is comparable to that observed in normal human intestinal tissue. There are different clones of Caco-2 cells that show a different expression in terms of hexoses transporters. Of these clones, we selected PD7 for presenting a high expression of the main transporters involved in the absorption of galactose at the intestinal level (SGLT1, GLUT2).

Cytotoxicity studies

In order to determine the possible toxicity of LPS and squalene on Caco-2 cells, cell viability studies were performed with the MTT technique. Cells were treated with/without 50 μM squalene and/or LPS 50 and 75 μg/ml for 24 hours. The results for MTT show that LPS and squalene do not affect cell viability at the tested concentrations as shown in Figure 5.

D-galactose uptake

Increased cell permeability leading to augmented intestinal absorption has been reported in states of sepsis caused by LPS [17]. In our experiments, after treating the cells with LPS and/or squalene for 24 h, 15-min absorption of 0.5 mM D-galactose was explored. The results showed that the absorption of sugar increased or decreased depending on the concentration of LPS assayed (Figure 6a). Concentrations lower than 50 μg/ml produced no effect on sugar transport (data not shown). Thus, a concentration of LPS 50 μg/ml caused a decrease in intestinal absorption while a high concentration of LPS (75 μg/ml) increased the sugar absorption. This concentration was required to reproduce the effect observed *in vivo*. These effects were suppressed in presence of 50 μM squalene confirming the animal data described above.

In this cell type, most of the SGLT1 transporter locates to the intracellular compartments and only a small amount is found in the apical membrane. Khoursandi et al. proposed a possible mechanism of regulation: in their hypothesis, the SGLT1 of the apical membrane would be inactivated after a period of time with respect to the transport capacity of D-glucose and then endocytosed. The endosomal SGLT1, in turn, would eventually be activated and return back to the plasma membrane. The entry of D-glucose sodium dependent to the cell could therefore be regulated without altering the cellular distribution of SGLT1 at steady state, by changes in the speed of the activation/inactivation cycle of SGLT1, which would ultimately determine the amount of transporter in the membrane [20].

Based on the results obtained in the absorption of D-galactose, we studied by Western blot the amount of SGLT1 protein in different cells conditions with/without squalene and/or LPS. The results showed a significant reduction in the expression of the SGLT1 transporter in the presence of 75 μg/ml LPS precisely when absorption is increased (Figure 6b). The effect of endotoxin was

suppressed by squalene. At 50 μm/ml LPS, the sugar transport is inhibited but the amount of SGLT1 protein was not modified. This event could indicate that at low LPS concentration, the SGLT1 intrinsic activity was modified. These results are in agreement with those previously obtained in rabbit jejunum.

By and large, according to these results, we can propose that high LPS doses increased D-galactose uptake through paracellular via but also decreased the active sugar transport because the SGLT1 levels were decreased. However, the endotoxin effect on paracellular way seems to be more important than on the transcellular route.

Thus, the increase in RELM-β expression observed which could be the cause of the decrease in SGLT1 levels. In this way, Krimi et al saw that RELM-β was able to decrease the activity and expression of SGLT1 in the brush border membrane [21].

On the other hand, the increased absorption of D-galactose by LPS observed may be due to an increase in MLCK protein since this protein is involved in cell permeability via paracellular. Several studies showed that LPS increases the permeability by tight junctions [17]. The increase in protein expression of MLCK would lead to an increase in MLC phosphorylation that would produce the contraction of the actin-myosin ring, thereby is increasing solute transport via paracellular. Likewise, it has been documented that LPS and IL-1β activate MLCK affecting cellular permeability [1].

At low doses, the LPS effect could be related to intrinsic activity of SGLT1. The activity of this protein can be modified by several factors, among which are proteins like MAPK and PI3K [19]. In this way, our group has shown in previous studies that these kinases are activated by the LPS [3,4].

Results docking

SGLT1 is a membrane glycoprotein localized in the brush border of the intestinal epithelium. The structure of rabbit or human SGLT1 proteins has not been resolved yet. For SGLT1, using Robetta software, one domain spanning amino acids 1 to 662 has been identified as a transmembrane one. This domain was identified as a protein transport and aligned to the structure of the K294A mutant of vSGLT (PDB 2XQ2) [39](amino acids 1 to 530) with a confidence of 0.6752. Within this domain, 5 different models were produced and validated using ProSA-web and ModEval. Validation

parameters are shown in Table S1. The predicted root-mean-squared deviation (RMSD) between the coordinates of the Cα atoms in the models and in the native structure was below 3 Å in all cases and at least 75% of Cα atoms were predicted to be within 3.5 Å of their positions in the native structure. GA341, a score for the reliability of the model, derived from statistical potentials, was higher than a pre-specified cut off (0.7) in all the cases. This fact indicates that the probability of the correct fold is larger than 95% in all obtained models. We also calculated z-DOPE and Z-score as parameters of protein model quality. Finally, based on the values obtained for z-score, RMSD and z-DOPE we selected model 5 for further analysis. For model 5, Ramachandran Plot was assessed, revealing that 94.4% of the residues were localized in favoured regions, 4.8% were in allowed regions and only 0.8% of all residues were placed in outlier regions (Figure S1A)

The structure of rabbit MLKC was also modelled using Robetta. In the first step, five domains were predicted (Table S2). Based on confidence level, *ab initio* and homology algorithms were used to model domain 1, whereas domains 2 to 5 were modelled by homology. After modelling the five domains, Robetta generated 5 different structures which were validated using ProSA-web and ModEval. Validation parameters are shown in Table S3. For all models, GA341, a score for the reliability of a model, was higher than a pre-specified cut off (0.7). Predicted RMSD between the coordinates of the Cα atoms in the models and in the native structure was above 3 Å in all cases and only in the case of model 2, and at least 75% of Cα atoms were predicted to be within 3.5 Å of their positions in the native structure. Finally, based on the values obtained for Z-score, RMSD and z-DOPE we selected model 2 for further analysis. For model 2 Ramachandran Plot was assessed, revealing that 94.4% of the residues were localized in favored regions, 4.8% were in allowed regions and only 0.8% were residues placed in outlier regions (Figure S1B).

Docking analysis of SGLT1

Docking between SGLT1 and squalene generated 32 different clusters of docking solutions concentrated in 6 different regions of the protein, while docking between SGLT1 and lipopolysaccharide produced 31 different clusters gathered in 5 different zones of the protein. To facilitate the study, for each region we selected the element whose interaction with the protein reported the most favourable ΔG. In consequence, we reduce the study to the analysis of 6 different ligand positions for the docking of SGLT1 and squalene and 5 different ligand positions for SGLT1 and lipopolysaccharide (Figure 7).

We used Chimera to analyze the interaction surfaces between the protein and the different docked ligands. We found 4 common interaction areas between lipopolysaccharide and squalene. In those areas, the estimated ΔG energy showed that the interaction between SGLT1 was more favorable than the interaction of SGLT1 with squalene (Table S3). We analyzed the different interactions that could be established between the SGLT1 and both ligands. Clashes and contact analyses did not report any interaction between any of the docked squalene and SGLT1. The same negative result was obtained for the docked lipopolysaccharide and SGLT1. We also used Chimera to find possible hydrogen bounds formed. Chimera showed that all docked lipopolysaccharide could form at least one hydrogen bound with SGLT1 whereas, any of the docked squalene reported any possible hydrogen bound formation with SGLT1 (3 and 4). The amino acids involved in these interactions are Lys 342 in Interaction Zone 2 (zone 1), Arg 52 and Arg 42 in Interaction Zone 2, Met 512 in Interaction Zone 3; Arg 259, Arg 564 and Trp 561 in Interaction Zone 4; Gln 253, Lys 254 in Interaction Zone 5.This fact explains the higher affinity of LPS for SGLT1. The amino acids involved in these interactions are Lys 342 in Interaction Zone 2 (zone 1), Arg 52 and Arg 42 in Interaction Zone 2, Met 512 in Interaction Zone 3; Arg 259, Arg 564 and Trp 561 in Interaction Zone 4; Gln 253, Lys 254 in Interaction Zone 5. (Figure S2)

SGLT1 functions as an active transporter for glucose. This protein transports one molecule of glucose inside the cells by cotransporting two molecules of Na^+. During this process, SGLT1 experiences a series of voltage- and ligand-induced conformational changes. For instance, the interaction of the inhibitor phlorizin with the C-terminal loop 13 of SGLT1 promotes major conformational changes in the protein that affects to its activity. On the other hand, interactions that involves the biding site for Na+ (Gly 43 and Arg 300) or for glucose (Gln 457) are expected to affect to the function of the protein (Consortium, 2017). In consequence, we analyse the capacity of LPS and squalene to interact with those regions. We found that both LPS and squalene can bind to SGLT1 in a region close to Arg 300 (Interaction Zone 2). Moreover, the obtained ΔG energy between LPS and SGLT1 in this area was the most favorable one. On the other hand, LPS, but not squalene can interact with the C-terminal loop 13 of SGLT1 although the affinity is lower than for Interaction Zone 2 (Figure S2).

Docking analysis of MLCK

Docking experiments was carried out with RossieLigand using model 2 MLCK structure as template and the ligand ZINC06845904 (squalene) and ZINC38377593 (lipopolysaccharide).

Solutions of docking MLCK-lipopolysaccharide, and docking MLCK-squalene were concentrated in just one region of the protein. Comparing both docking, both ligand share a common interaction. In this area, the estimated ΔG energy showed that the interaction between MLCK and lipopolysaccharide was more favourable than the interaction of MLCK with squalene (Table S4).

Interaction surfaces between the protein and the different docked ligands were analysed using Chimera. Clashes and contact analyses did not report any interaction between any of the docked squalene and MLCK. The same negative result was obtained for the docked lipopolysaccharide and MLCK. We also used Chimera to find possible hydrogen bounds formed between MLCK and both ligands. Chimera showed that all docked lipopolysaccharide could form at least one hydrogen bound with MLCK whereas, any of the docked squalene reported any possible hydrogen bound formation with MLCK (Figure 8).

In both cases, the amino acids that could be involved in the binding between the protein and the ligands are Val 116, Glu 133, Thr 124, Leu 125, Lys 126, Ile 221, Asn 223, Lys 658 and Glu 660. Most of the amino acids involved in the binding area are placed in the actin binding domain, whereas the proton acceptor of the active centre (Asp 817) and the amino acids involved in the ATP binding (Lys 125) seem not to be involved in the binding zone.

In addition, the results obtained by bioinformatic analysis indicate a possible interaction between squalene and LPS with the binding site for Na^+ of the SGLT1 transporter, which modified its intrinsic activity. Perhaps it seems that in the case of LPS, a slight interaction could be given, which added to the aforementioned by the action of the kinases, could modify the affinity of the transporter for sugar, a fact that could occur in the case of low doses or concentrations of endotoxin.

Likewise, bioinformatic studies have shown an area of interaction between SGLT1 and RELM-β that could affect the transporter.

On the other hand, it was observed that the sugar absorption in the group with LPS but fed with the feed supplemented to 0.5% squalene was not increased.

Through bioinformatic studies, it was observed that squalene could interact with the active site of MLCK and this event could affect the functionality of the kinase. But in what way does squalene cancel the effect of LPS?

Previous studies carried out by our group on rabbits and Caco-2 cells have shown that LPS, TNF-α and IL-1β inhibit the intestinal absorption of D-fructose and D-galactose by modifying the activity or capacity of transport of GLUT5 or SGLT1 through the activation of intracellular pathways in which kinase proteins are involved, such as PKC, PI3K, MAPKk's and nuclear transcription factor (NF-kB) [13-15].

In addition, several studies relate the anti-inflammatory effect of the hydrocarbon polyphenols (squalene), β -carotenes, etc. of virgin olive oil with the inactivation of NF-kB [28]. Therefore, perhaps squalene could cancel the effect of LPS by inactivating NF-kB, but future studies in this regard should be done.

In summary, squalene could reversed the effect of LPS through its interaction with MLCK and NF- kB. In addition, bioinformatic studies confirm the interaction between LPS-squalene through the MLCK and SGLT1 proteins.

Acknowledgment

This work was supported by grants from Grants from Ministerio de Economia y Competitividad, Gobierno de España (SAF2016-75441-R), CIBERobn (CB06/03/1012), Gobierno de Aragón (A-32, B-69), and SUDOE (Redvalue, SOE1/PI/E0123). Molecular graphics and analyses were performed with the UCSF Chimera package. Chimera is developed by the Resource for Biocomputing, Visualization, and Informatics at the University of California, San Francisco (supported by NIGMS P41-GM103311).

Conflict of interest

The authors declare that they have no copeting interests.

References

1. Al-Sadi R, Guo S, Dokladny K, Smith MA, Ye D, Kaza A, Watterson DM, Ma TY (2012) Mechanism of interleukin-1beta induced-increase in mouse intestinal permeability in vivo. J Interferon Cytokine Res 32:474-484. doi:10.1089/jir.2012.0031
2. Al-Sadi R, Guo S, Ye D, Rawat M, Ma TY (2016) TNF-alpha Modulation of Intestinal Tight Junction Permeability Is Mediated by NIK/IKK-alpha Axis Activation of the Canonical NF-kappaB Pathway. Am J Pathol 186:1151-1165. doi:S0002-9440(16)00077-8 [pii]
10.1016/j.ajpath.2015.12.016
3. Amador P, Garcia-Herrera J, Marca MC, de la Osada J, Acin S, Navarro MA, Salvador MT, Lostao MP, Rodriguez-Yoldi MJ (2007) Inhibitory effect of TNF-alpha on the intestinal absorption of galactose. J Cell Biochem 101:99-111. doi:10.1002/jcb.21168
4. Amador P, Marca MC, Garcia-Herrera J, Lostao MP, Guillen N, de la Osada J, Rodriguez-Yoldi MJ (2008) Lipopolysaccharide induces inhibition of galactose intestinal transport in rabbits in vitro. Cell Physiol Biochem 22:715-724. doi:000185555 [pii]
10.1159/000185555
5. Berkes J, Viswanathan VK, Savkovic SD, Hecht G (2003) Intestinal epithelial responses to enteric pathogens: effects on the tight junction barrier, ion transport, and inflammation. Gut 52:439-451
6. Cardeno A, Magnusson MK, Strid H, Alarcon de La Lastra C, Sanchez-Hidalgo M, Ohman L (2014) The unsaponifiable fraction of extra virgin olive oil promotes apoptosis and attenuates activation and homing properties of T cells from patients with inflammatory bowel disease. Food Chem 161:353-360. doi:S0308-8146(14)00560-3 [pii]
10.1016/j.foodchem.2014.04.016
7. Clayburgh DR, Rosen S, Witkowski ED, Wang F, Blair S, Dudek S, Garcia JG, Alverdy JC, Turner JR (2004) A differentiation-dependent splice variant of myosin light chain kinase, MLCK1, regulates epithelial tight junction permeability. J Biol Chem 279:55506-55513. doi:M408822200 [pii]
10.1074/jbc.M408822200
8. Chantret I, Rodolosse A, Barbat A, Dussaulx E, Brot-Laroche E, Zweibaum A, Rousset M (1994) Differential expression of sucrase-isomaltase in clones isolated from early and late passages of the cell line Caco-2: evidence for glucose-dependent negative regulation. J Cell Sci 107 (Pt 1):213-225
9. Choudhry N, Bajaj-Elliott M, McDonald V (2008) The terminal sialic acid of glycoconjugates on the surface of intestinal epithelial cells activates excystation of Cryptosporidium parvum. Infect Immun 76:3735-3741. doi:IAI.00362-08 [pii]
10.1128/IAI.00362-08
10. Dawson DJ, Burrows PC, Lobley RW, Holmes R (1987) The kinetics of monosaccharide absorption by human jejunal biopsies: evidence for active and passive processes. Digestion 38:124-132. doi:10.1159/000199581
11. DeLuca S, Khar K, Meiler J (2015) Fully Flexible Docking of Medium Sized Ligand Libraries with RosettaLigand. PLoS One 10:e0132508. doi:10.1371/journal.pone.0132508
PONE-D-15-06401 [pii]

12. Ferraris RP, Diamond J (1997) Regulation of intestinal sugar transport. Physiol Rev 77:257-302. doi:10.1152/physrev.1997.77.1.257
13. Garcia-Barrios A, Guillen N, Gascon S, Osada J, Vazquez CM, Miguel-Carrasco JL, Rodriguez-Yoldi MJ (2010) Nitric oxide involved in the IL-1beta-induced inhibition of fructose intestinal transport. J Cell Biochem 111:1321-1329. doi:10.1002/jcb.22859
14. Garcia-Herrera J, Marca MC, Brot-Laroche E, Guillen N, Acin S, Navarro MA, Osada J, Rodriguez-Yoldi MJ (2008) Protein kinases, TNF-{alpha}, and proteasome contribute in the inhibition of fructose intestinal transport by sepsis in vivo. Am J Physiol Gastrointest Liver Physiol 294:G155-164. doi:00139.2007 [pii]
10.1152/ajpgi.00139.2007
15. Garcia-Herrera J, Navarro MA, Marca MC, de la Osada J, Rodriguez-Yoldi MJ (2004) The effect of tumor necrosis factor-alpha on D-fructose intestinal transport in rabbits. Cytokine 25:21-30. doi:S104346660300320X [pii]
16. Grosdidier A, Zoete V, Michielin O (2011) Fast docking using the CHARMM force field with EADock DSS. J Comput Chem 32:2149-2159. doi:10.1002/jcc.21797
17. Guo S, Al-Sadi R, Said HM, Ma TY (2012) Lipopolysaccharide causes an increase in intestinal tight junction permeability in vitro and in vivo by inducing enterocyte membrane expression and localization of TLR-4 and CD14. Am J Pathol 182:375-387. doi:S0002-9440(12)00808-5 [pii]
10.1016/j.ajpath.2012.10.014
18. Hecht G, Koutsouris A (1999) Enteropathogenic E. coli attenuates secretagogue-induced net intestinal ion transport but not Cl- secretion. Am J Physiol 276:G781-788
19. Helliwell PA, Richardson M, Affleck J, Kellett GL (2000) Regulation of GLUT5, GLUT2 and intestinal brush-border fructose absorption by the extracellular signal-regulated kinase, p38 mitogen-activated kinase and phosphatidylinositol 3-kinase intracellular signalling pathways: implications for adaptation to diabetes. Biochem J 350 Pt 1:163-169
20. Khoursandi S, Scharlau D, Herter P, Kuhnen C, Martin D, Kinne RK, Kipp H (2004) Different modes of sodium-D-glucose cotransporter-mediated D-glucose uptake regulation in Caco-2 cells. Am J Physiol Cell Physiol 287:C1041-1047. doi:10.1152/ajpcell.00197.2004
00197.2004 [pii]
21. Krimi RB, Letteron P, Chedid P, Nazaret C, Ducroc R, Marie JC (2009) Resistin-like molecule-beta inhibits SGLT-1 activity and enhances GLUT2-dependent jejunal glucose transport. Diabetes 58:2032-2038. doi:db08-1786 [pii]
10.2337/db08-1786
22. Lou-Bonafonte JM, Arnal C, Navarro MA, Osada J (2012) Efficacy of bioactive compounds from extra virgin olive oil to modulate atherosclerosis development. Mol Nutr Food Res 56:1043-1057. doi:10.1002/mnfr.201100668
23. Lou-Bonafonte JM, Martinez-Beamonte R, Sanclemente T, Surra JC, Herrera-Marcos LV, Sanchez-Marco J, Arnal C, Osada J (2018) Current Insights into the Biological Action of Squalene. Mol Nutr Food Res:e1800136. doi:10.1002/mnfr.201800136

24. Ma TY, Anderson JM (2012) Tight Junctions and the intestinal barrier. Inc: Physiology of the Gastrointestinal Tract., Burlingtong, MA: Elsevier Academic Press.
25. Nighot M, Al-Sadi R, Guo S, Rawat M, Nighot P, Watterson MD, Ma TY (2017) Lipopolysaccharide-Induced Increase in Intestinal Epithelial Tight Permeability Is Mediated by Toll-Like Receptor 4/Myeloid Differentiation Primary Response 88 (MyD88) Activation of Myosin Light Chain Kinase Expression. Am J Pathol 187:2698-2710. doi:S0002-9440(17)30306-1 [pii]
10.1016/j.ajpath.2017.08.005
26. Pettersen EF, Goddard TD, Huang CC, Couch GS, Greenblatt DM, Meng EC, Ferrin TE (2004) UCSF Chimera--a visualization system for exploratory research and analysis. J Comput Chem 25:1605-1612. doi:10.1002/jcc.20084
27. Reboredo-Rodriguez P, Varela-Lopez A, Forbes-Hernandez TY, Gasparrini M, Afrin S, Cianciosi D, Zhang J, Manna PP, Bompadre S, Quiles JL, Battino M, Giampieri F (2018) Phenolic Compounds Isolated from Olive Oil as Nutraceutical Tools for the Prevention and Management of Cancer and Cardiovascular Diseases. Int J Mol Sci 19. doi:ijms19082305 [pii]
10.3390/ijms19082305
28. Sanchez-Fidalgo S, Villegas I, Aparicio-Soto M, Cardeno A, Rosillo MA, Gonzalez-Benjumea A, Marset A, Lopez O, Maya I, Fernandez-Bolanos JG, Alarcon de la Lastra C (2015) Effects of dietary virgin olive oil polyphenols: hydroxytyrosyl acetate and 3, 4-dihydroxyphenylglycol on DSS-induced acute colitis in mice. J Nutr Biochem 26:513-520. doi:S0955-2863(15)00015-7 [pii]
10.1016/j.jnutbio.2014.12.001
29. Sanchez-Fidalgo S, Villegas I, Rosillo MA, Aparicio-Soto M, de la Lastra CA (2014) Dietary squalene supplementation improves DSS-induced acute colitis by downregulating p38 MAPK and NFkB signaling pathways. Mol Nutr Food Res 59:284-292. doi:10.1002/mnfr.201400518
30. Shirazi-Beechey SP (1995) Molecular biology of intestinal glucose transport. Nutr Res Rev 8:27-41. doi:S0954422495000060 [pii]
10.1079/NRR19950005
31. Simons KT, Kooperberg C, Huang E, Baker D (1997) Assembly of protein tertiary structures from fragments with similar local sequences using simulated annealing and Bayesian scoring functions. J Mol Biol 268:209-225. doi:S0022-2836(97)90959-1 [pii]
10.1006/jmbi.1997.0959
32. Song Y, DiMaio F, Wang RY, Kim D, Miles C, Brunette T, Thompson J, Baker D (2013) High-resolution comparative modeling with RosettaCM. Structure 21:1735-1742. doi:S0969-2126(13)00297-9 [pii]
10.1016/j.str.2013.08.005
33. Tsukita S, Furuse M, Itoh M (2001) Multifunctional strands in tight junctions. Nat Rev Mol Cell Biol 2:285-293. doi:10.1038/35067088
35067088 [pii]
34. Turner JR (2009) Intestinal mucosal barrier function in health and disease. Nat Rev Immunol 9:799-809. doi:nri2653 [pii]
10.1038/nri2653
35. van Meerloo J, Kaspers GJ, Cloos J (2011) Cell sensitivity assays: the MTT assay. Methods Mol Biol 731:237-245. doi:10.1007/978-1-61779-080-5_20

36. Vayro S, Wood IS, Dyer J, Shirazi-Beechey SP (2001) Transcriptional regulation of the ovine intestinal Na+/glucose cotransporter SGLT1 gene. Role of HNF-1 in glucose activation of promoter function. Eur J Biochem 268:5460-5470. doi:ejb2488 [pii]
37. Veyhl M, Keller T, Gorboulev V, Vernaleken A, Koepsell H (2006) RS1 (RSC1A1) regulates the exocytotic pathway of Na+-D-glucose cotransporter SGLT1. Am J Physiol Renal Physiol 291:F1213-1223. doi:00068.2006 [pii]
10.1152/ajprenal.00068.2006
38. Warleta F, Campos M, Allouche Y, Sanchez-Quesada C, Ruiz-Mora J, Beltran G, Gaforio JJ (2010) Squalene protects against oxidative DNA damage in MCF10A human mammary epithelial cells but not in MCF7 and MDA-MB-231 human breast cancer cells. Food Chem Toxicol 48:1092-1100. doi:S0278-6915(10)00083-9 [pii]
10.1016/j.fct.2010.01.031
39. Watanabe A, Choe S, Chaptal V, Rosenberg JM, Wright EM, Grabe M, Abramson J (2010) The mechanism of sodium and substrate release from the binding pocket of vSGLT. Nature 468:988-991. doi:nature09580 [pii]
10.1038/nature09580
40. Wiederstein M, Sippl MJ (2007) ProSA-web: interactive web service for the recognition of errors in three-dimensional structures of proteins. Nucleic Acids Res 35:W407-410. doi:gkm290 [pii]
10.1093/nar/gkm290
41. Xu J, Liu Z, Zhan W, Jiang R, Yang C, Zhan H, Xiong Y (2018) Recombinant TsP53 modulates intestinal epithelial barrier integrity via upregulation of ZO1 in LPSinduced septic mice. Mol Med Rep 17:1212-1218. doi:10.3892/mmr.2017.7946
42. Yu LC, Turner JR, Buret AG (2006) LPS/CD14 activation triggers SGLT-1-mediated glucose uptake and cell rescue in intestinal epithelial cells via early apoptotic signals upstream of caspase-3. Exp Cell Res 312:3276-3286. doi:S0014-4827(06)00251-5 [pii]
10.1016/j.yexcr.2006.06.023

Legends of the figures

Figure 1. Temperature increase of rabbit treated with 6 μg/kg bw LPS for 90 min. Control: animals without squalene diet. Squalene: animals with squalene diet. *p<0.05 with respect to control animals.

Figure 2. Body temperature of rabbit fed with/without squalene and treated with 1 mg/kg bw LPS for one week. Control: animals without squalene diet. LPS: animals without squalene diet and treated with LPS. LPS/Squalene: animals with squalene diet and treated with LPS. *p<0.05 with respect to control animals. #p<0.05 with respect to LPS animals.

Figure 3. *Absorption of D-galactose in the acute LPS effect*: a) Effect of the administration of LPS 6 μg/kg bw on intestinal absorption of 0.5 mM D-galactose in rabbits with control diet or diet with a squalene (SQL) supplement. The incubation time was 3 min. The results were obtained from 6 animals per condition with 12 determinations per animal. *p<0.05 with respect to control animals. #p<0.05 with respect to LPS animals. *Protein study by western blot*. The information is given as protein expression intensity (mean ± SEM in arbitrary units (AU) normalized with its actin. b) SGLT1 expression. c) RELM-β expression. d) MLCK expression. *p<0.05 with respect to control animals.

Figure 4. *Absorption of D-galactose in the chronic LPS effect:* a) Effect of the administration of LPS 1 mg/kg bw on intestinal absorption of 0.5 mM D-galactose in rabbits with control diet or diet with a squalene (SQL) supplement. The incubation time was 3 min. The results were obtained from 6 animals per condition with 12 determinations per animal. *p<0.05 with respect to control animals. #p<0.05 with respect to LPS animals. Protein study by western blot. The information is given as protein expression intensity (mean ± SEM) in arbitrary units (AU) normalized to actin. b) SGLT1 expression. c) RELM-β expression. d) MLCK expression. *p<0.05 with respect to control animals. #p<0.05 with respect to LPS animals.

Figure 5. Study of the cytotoxicity (MTT) of squalene (SQL) 50 μM and LPS at the concentration 50 and 75 μg/ml on Caco-2 cells. The results are given as absorbance values. The number of determinations was 12.

Figure 6. *Uptake of D-galactose in Caco-2 cells under different conditions*: a) Absorption of 0.5 mM D-galactose in the absence (control) or presence of 50 and 75 μg/ml LPS and/or 50 μM squalene after 24 h of preincubation time. Incubation time with sugar 15 min. N = 12 in each condition. *p<0.05 with respect to control animals. Protein study by western blot. The information is given as protein expression intensity (mean ± SEM) in arbitrary units (AU) normalized to actin expression. b) SGLT1 expression.*p<0.05 with respect to control animals.

Figure 7. Docking analysis. Visualization of the predicted interaction areas between SGLT1 and LPS (purple) and between SGLT1 and squalene (green). We also represented the biding site for glucose (Gln 457) in red, for Na^+ (Arg 300 and Gly 43) in orange, and for inhibitors (loop 13) in blue.

Figure 8. Analysis of the four interaction zones of MLCK with lipopolysaccharide (in grey) and squalene (in green).

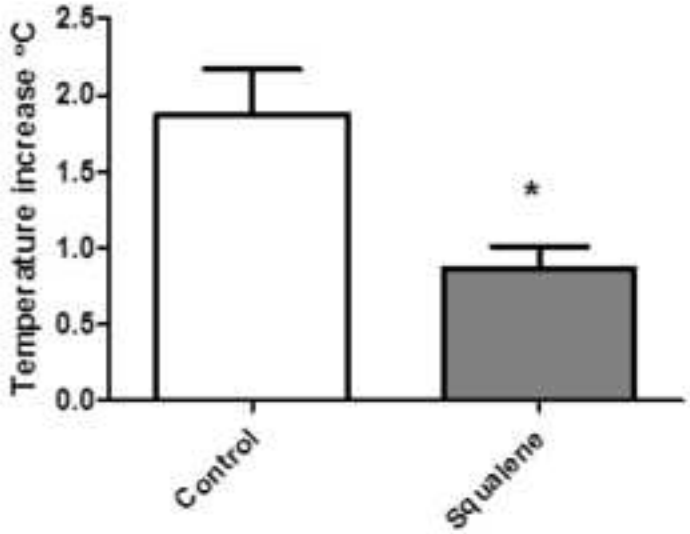

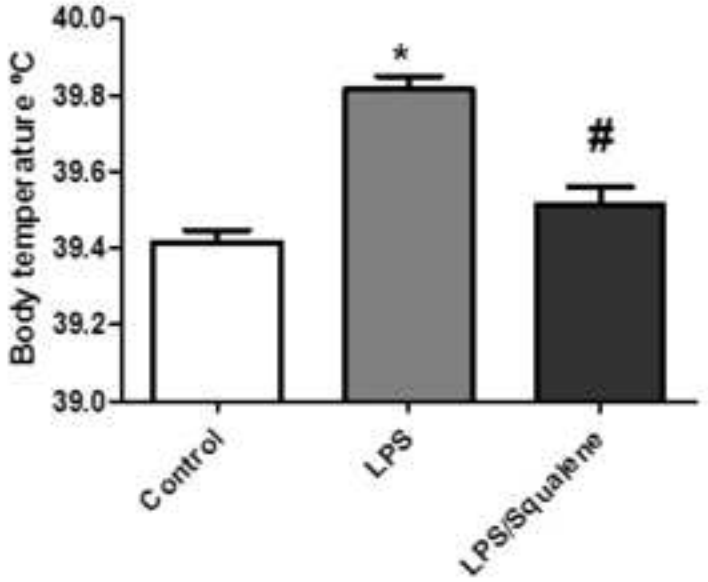

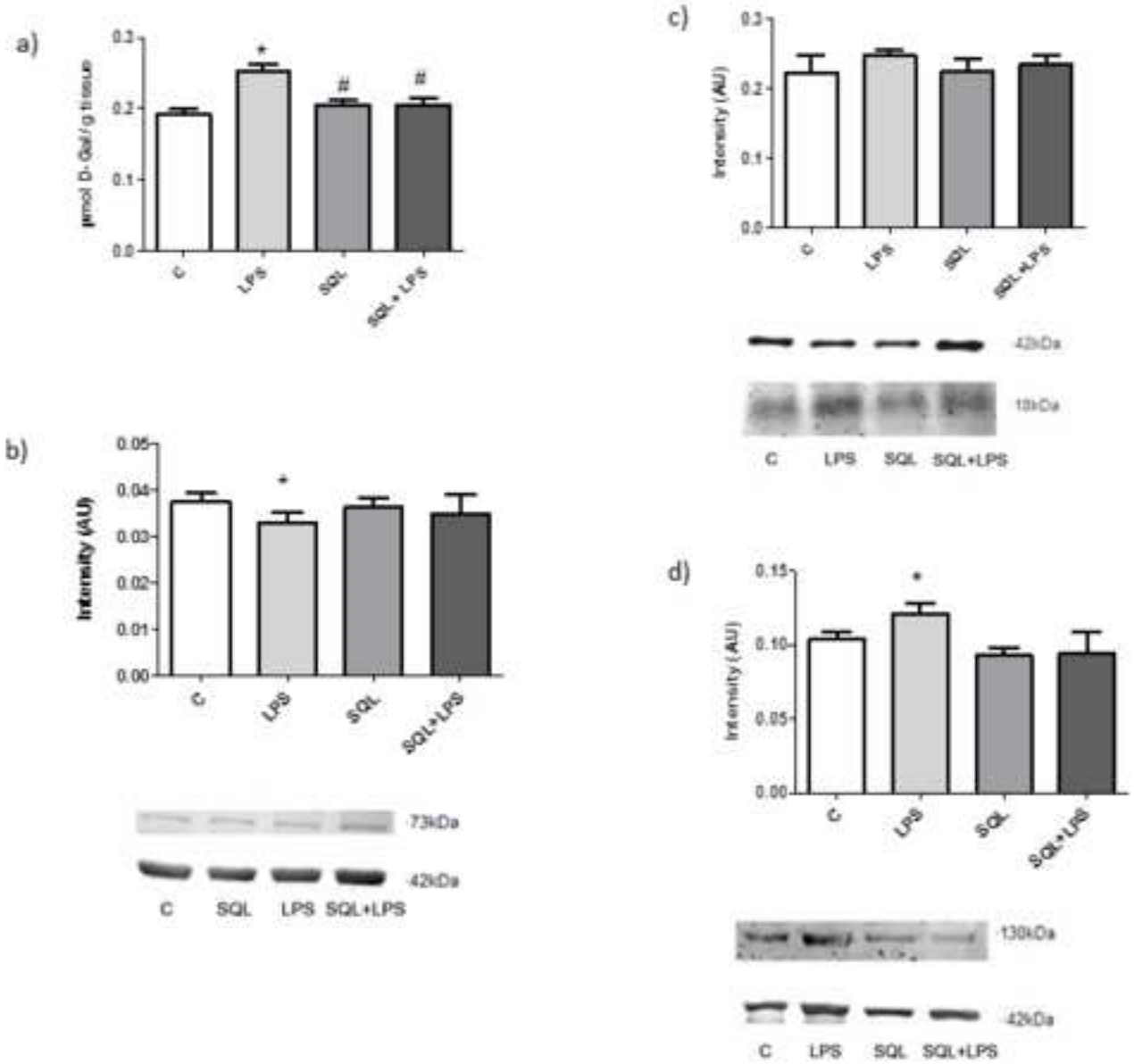

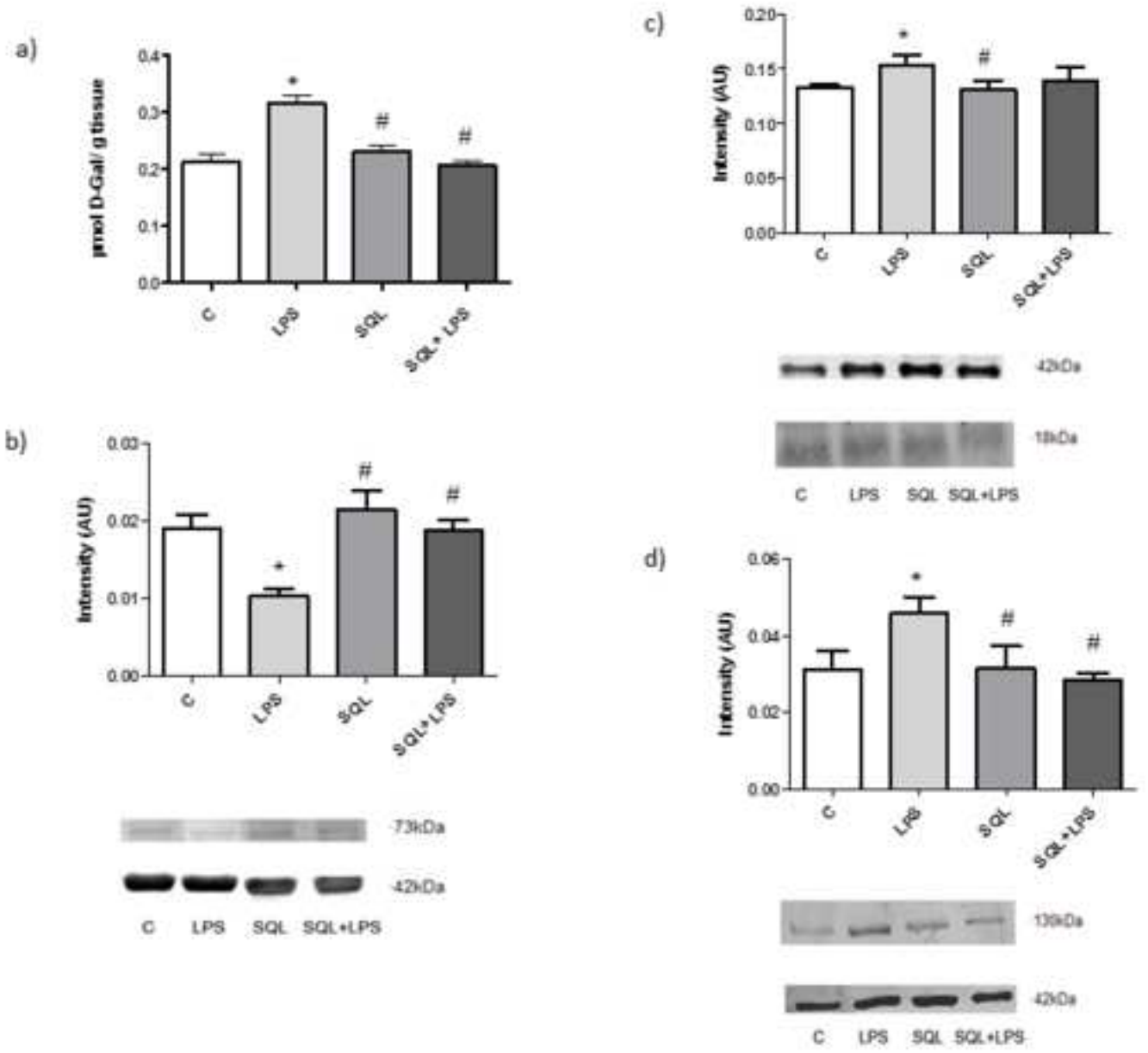

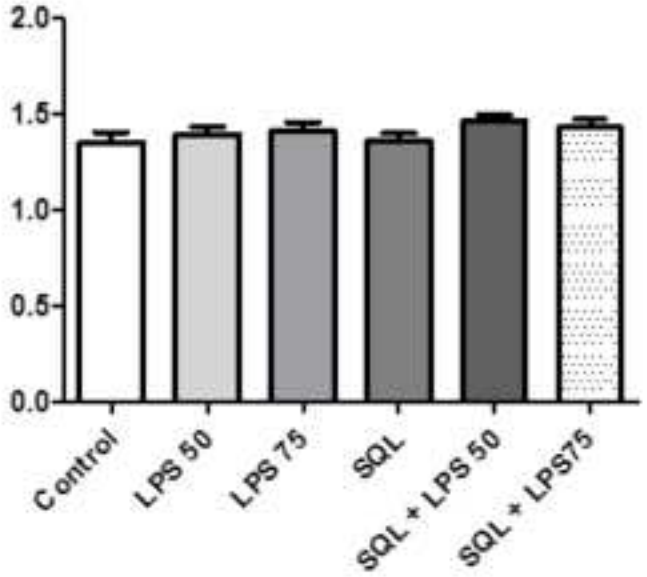

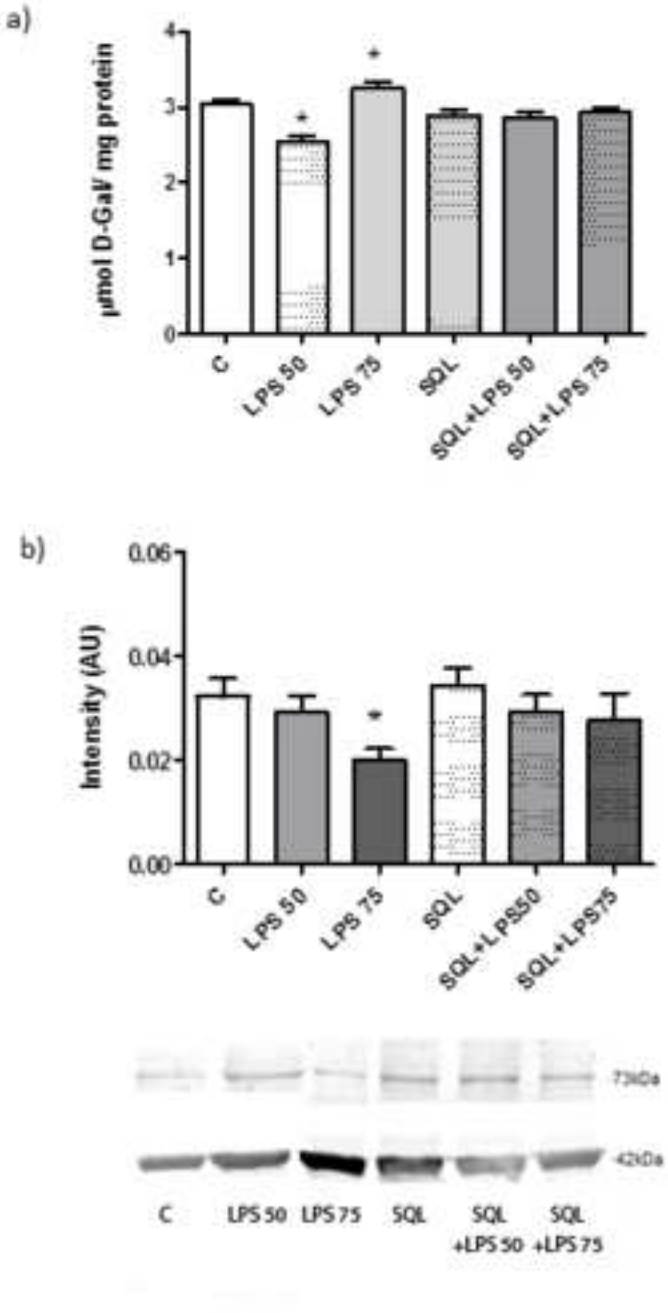

Table S1. Validation parameters for the 5 models of SGLT1 produced by Robetta.

Model number	Overall model quality z-score	Predicted RMSD	Predicted Native Overlap (3.5 Å)	z-DOPE	GA341
1	-6.96	3.00 Å	0.757	-1.517	1
2	-6.58	2.76 Å	0.761	-1.429	1
3	-6.62	3.00 Å	0.810	-1.374	1
4	-6.72	2.99 Å	0.774	-1.391	1
5	-7.10	2.85 Å	0.777	-1.462	1

Table S2. Domains of rabbit MLKC predicted by Ginzu.

Domain	Span	Source	Reference Parent	Parent Span	Confidence	Anotations
1	160-224	Msa	4v5zBg	1-48	0.197	-
2	225-424	Alignment	3b43A (von Castelmur et al., 2008)	1-569	0.976	Structural protein
3	425-680	Alignment	4yfdA (Yamagata et al., 2015)	1-491	0.722	-
4	681-995	Alignment	1kobA(Kobe et al., n.d.)	1-353	0.830	Kinase
5	996-1147	Alignment	2rikA (von Castelmur et al., 2008)	1-283	0.673	Structural protein

Table S3. Validation parameters for the 5 models of SGLT1 produced by Robetta.

Model number	Overall model quality z-score	Predicted RMSD	Predicted Native Overlap (3.5 Å)	z-DOPE	GA341
1	-3.14	6.609	0.534	-0.065	1
2	-3.07	3.951	0.785	-0.392	1
3	-3.54	5.846	0.654	-0.207	1
4	-2.78	5.240	0.679	-0.290	1
5	-3.27	5.687	0.626	-0.234	1

Table S4. Estimation of ΔG energy value for the interactions of SGLT1 with LPS and SQL. Interaction zone numbers were assigned randomly

Interaction zone	LPS ligand		SQL ligand	
	Name	ΔG (Kcal/mol)	Name	ΔG (Kcal/mol)
1	LIG 2	-9.123	LIG 6	-8.057
2	LIG 3	-10.623	LIG 3	-7.986
3	LIG 4	-8.605	LIG 2	-8.488
4	LIG 5	-10.387	LIG 1	-7.972
5	LIG 1	-8.983	-	-
6	-	-	LIG 4	-8.198
7	-	-	LIG 5	-7.350

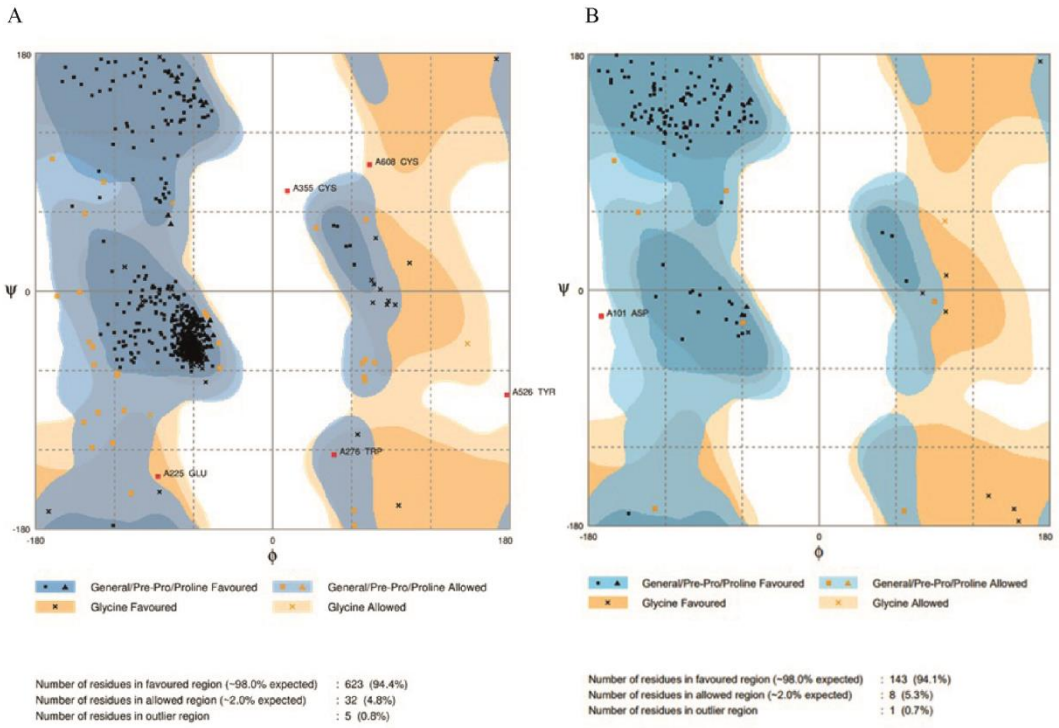

Figure S1. Ramachandran Plot for (A) SGLT1 model 5 and (B) MLCK model 2.

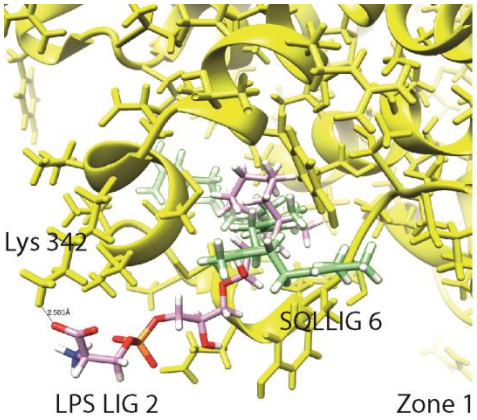
Lys 342
SQLLIG 6
LPS LIG 2
Zone 1

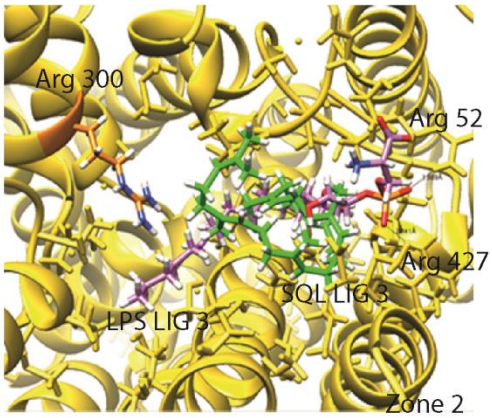
Arg 300
Arg 52
Arg 427
SQL LIG 3
LPS LIG 3
Zone 2

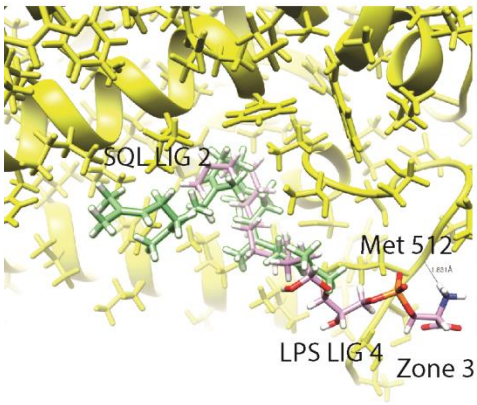
SQL LIG 2
Met 512
LPS LIG 4
Zone 3

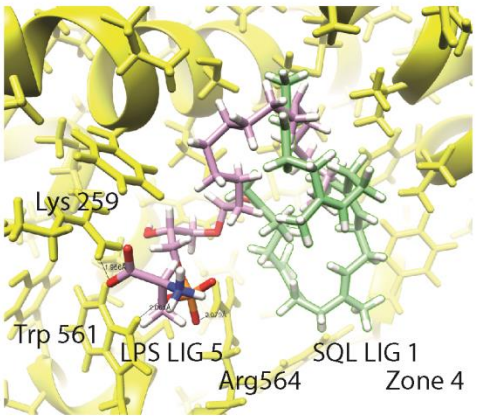
Lys 259
Trp 561
LPS LIG 5
SQL LIG 1
Arg564
Zone 4

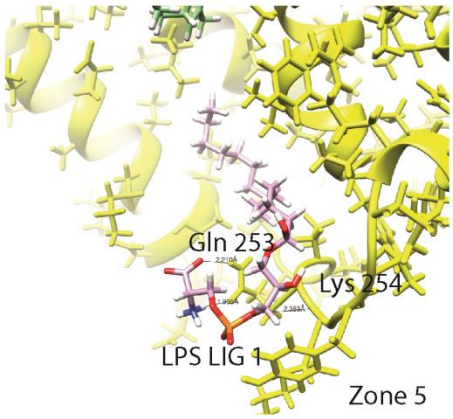
Gln 253
Lys 254
LPS LIG 1
Zone 5

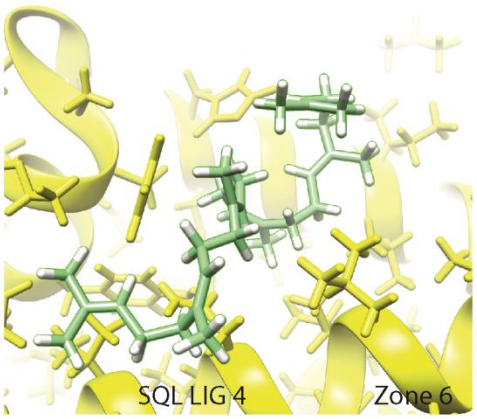
SQL LIG 4
Zone 6

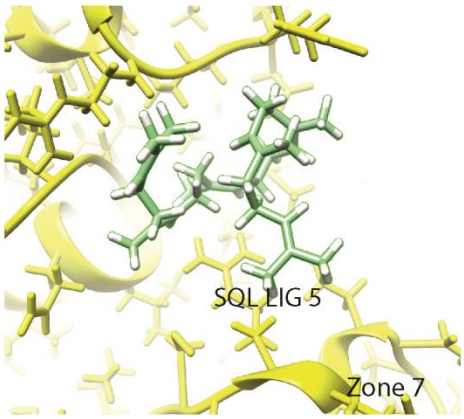
SQL LIG 5
Zone 7

Figure S2. Analysis of the six interaction zones of SGTL1 with Lipopolysacharide (in purple) and squalene (in green). Possible hydrogen bond stablished between SGLT1 and the different ligands are represented as black bonds and the distance between the clashed atoms is shown in Amstroms. (A) Zone 1, interaction of SGLT1 with LPS ligand 2 (-9.123 Kcal/mol) and SQL ligand 6 (-8.057 Kcal/mol); (B) Zone 2, interaction of SGLT1 with LPS ligand 3 (-10.623 Kcal/mol) and SQL ligand 3 (-7.986 Kcal/mol); (C) Zone 3, interaction of SGLT1 with LPS ligand 4 (-8.605 Kcal/mol) and SQL ligand 2 (-8.488 Kcal/mol); (D) Z;one 4, interaction of SGLT1 with LPS ligand 5 (-10.387 Kcal/mol) and SQL ligand 1 (-7.972 Kcal/mol); (E) Zone 5, interaction of SGLT1 with LPS ligand 1 (-8.983 Kcal/mol) (F) Zone 6, interaction of SGLT1 with SQL ligand 4 (-8.198 Kcal/mol); (G) Zone interaction of SGLT1 with SQL ligand 5 (-7.350 Kcal/mol). We also represented the biding site for Na^+ (Arg 300) in orange.